

To appear in *Molecular Simulation*
Vol. 00, No. 00, Month 20XX, 1–14

Coarse-Grained Simulations of Modified Jeffamine ED900 Micelles

Fabián A. García Daza and Allan D. Mackie*

Departament d'Enginyeria Química, ETSEQ, Universitat Rovira i Virgili, Avinguda dels Països Catalans 26, 43007 Tarragona, Spain

(Received 00 Month 20XX; final version received 00 Month 20XX)

A coarse-grained model is presented for the gemini block copolymer surfactant $C_{13}H_{27}CONH-PO_3-EO_{12.5}-PO_3-NHCOC_{13}H_{27}$, otherwise known by its trade name Jeffamine ED900Myr, used in the preparation of ordered mesoporous materials. From Single-Chain Mean-Field simulations, we find that the surfactant is able to form spherical micelles whose structure is qualitatively similar to experimental data. The critical micelle concentration, however, is orders of magnitude lower than the one reported experimentally. This discrepancy between calculated and experimental critical micelle concentrations has previously been observed for other strongly hydrophobic surfactant systems and suggests the presence of non-equilibrium effects in the experimental system. By taking the kinetic effects into account in the formation of the micelles, an apparent critical micelle concentration is found which is quantitatively similar to the experimental value.

Keywords: Mean-field theory, copolymer surfactants, micelles, self-assembly, coarse-grained model

1. Introduction

Surfactants are amphiphilic molecules with hydrophilic and hydrophobic moieties that interact favourably and unfavourably with the surrounding solvent, respectively. Because of this particular characteristic, surfactants are able to self-organise into well-defined geometric structures above a concentration known as the critical micelle concentration (CMC). Over the last decades, surfactants have appealed to researchers who have attempted to maximise their versatility for a broad range of applications including: drug capture, transport and delivery mechanisms [1], waste water purification treatments [2], hydrogel synthesis [3], design of biological materials [4] and nanotechnology development [5]. More recently, surfactants have been widely explored as templates for the synthesis of mesoporous silica materials [6–10] whose dimensions and properties can be controlled by modifying the chemical and physical properties of the surfactants. Depending on the experimental conditions, two common methods are found for synthesizing mesoporous materials. At high surfactant concentrations, liquid crystal can be used to set up the building blocks of the materials whereas at low concentrations micellar phases are employed.

A significant number of theoretical works can be found in the literature that attempt to model these templating systems. For instance, free energy models [11, 12] based on the different free energy contributions are able to describe important equilibrium properties such as the CMC, micellar shape or phase behaviour. Unfortunately, there is a lack of explicit microscopic information given the semi-empirical foundations of this approach. Conventional simulation techniques like Monte Carlo (MC) [13] and molecular dynamics (MD) [14, 15] have been applied to study the aggregation process for several kind of surfactant molecules. Nevertheless, equilibration problems have been reported even for coarse-grained models of short nonionic surfactants, affecting the comparison

*Corresponding author. Email: allan.mackie@urv.cat

of equilibrium properties like the aggregate size distribution or the CMC with experimental data [15]. Alternative mean-field methods have also been considered where the system's free energy is formulated in terms of a set of sampling chains representing the surfactant, to be later minimised ensuring an equilibrium regime. For example, the self-consistent field (SCF) [16] and single-chain mean-field (SCMF) [17, 18] theories have been used to study block copolymer surfactants and have proven to be efficient tools in the prediction of equilibrium properties. In both cases, the intermolecular interactions are expressed by mean molecular fields. However, the SCF theory considers the presence of overlapping conformations. This assumption affects the intramolecular energy given the absence of excluded-volume interactions. Contrary to this, the SCMF theory can take into account non-Markovian conformations by only including self-avoiding configurations in the set of sampling chains. This leads to more realistic surfactant models and, in consequence, more precise estimates of the system's free energy. The results obtained by the SCMF theory have been compared with Monte Carlo simulation [17] as well as with available experimental data such as the CMC, as in the case of nonionic gemini surfactants [19], diblock poly(ethylene oxide) alkyl ether surfactants (C_nEO_m) [18], and, poly(ethylene oxide)-poly(propylene oxide)-poly(ethylene oxide) block copolymers ($EO_mPO_nEO_m$) [20].

Given the increasing interest to formulate mesoporous structures based on surfactant copolymers with large molecular weights, this work is devoted to the development and simulation of a coarse-grained model at 25 °C for the gemini surfactant $C_{13}H_{27}CONH-PO_3-EO_{12.5}-PO_3-NHCOC_{13}H_{27}$, also known as ED900Myr, which has been synthesised by May and co-workers [8]. This surfactant has been used as a molecular sieve for the preparation of ordered mesoporous materials. In the following Methodology section the fundamentals of the SCMF theory and the connection with macroscopic observables are described. In addition, the surfactant coarse-grained model and the energetic parameters are introduced and details of the fitting procedure are given. In the Results and Discussion section, the CMC and micellar structural properties are compared with the available experimental data. An explanation is given of the discrepancy found between the experimental CMC and the one obtained by our simulations. This discrepancy is expected for very hydrophobic surfactants [19–22] such as the one studied in this work and is discussed within a kinetics micellization framework combined with the SCMF results. The article finishes with a section on the main conclusions of this work.

2. Methodology

2.1. The Single-Chain Mean-Field Theory

The SCMF theory [17, 18, 20, 23, 24] is based on a central chain, α , whose intermolecular interactions are described by molecular mean fields of other chains and solvent, whereas the intramolecular contributions are obtained in an exact manner. These intermolecular fields are determined self-consistently. The starting point of the theory is to consider the free energy of a system of N physical chains in terms of the individual contributions from a set of sampling chains $\{\alpha\}$,

$$F = N \int \mathcal{D}\alpha P[\alpha] U[\alpha] + kT \int d\mathbf{r} c_S(\mathbf{r}) \log \phi_S(\mathbf{r}) + NkT \int \mathcal{D}\alpha P[\alpha] \log P[\alpha], \quad (1)$$

where k , T and $P[\alpha]$ are the Boltzmann constant, the temperature of the system and the probability associated with conformation α , respectively. The term $U[\alpha]$ on the right hand side of the above equation represents the intra and intermolecular energies of chain α with other conformations and solvent. The solvent medium, denoted as S , is represented by its concentration fields $c_S(\mathbf{r})$ and is related with the volume fraction by $\phi_S(\mathbf{r}) = v_S c_S(\mathbf{r})$ where v_S is the volume of a solvent monomer. The second and third terms are the translational and conformational entropies of solvent and chain

molecules.

The equilibrium solution of the system can be found by minimising the free energy given in Equation 1 with respect to the chain probabilities $P[\alpha]$ and the solvent concentration $c_S(\mathbf{r})$. A set of Lagrange multipliers are used in order to include the volume-filling constraints which ensure that the space is occupied by either solvent or chain molecules,

$$\phi_S(\mathbf{r}) + N \sum_i \langle \phi_i(\mathbf{r}) \rangle = 1, \quad (2)$$

where, $\langle \phi_i(\mathbf{r}) \rangle$ is the average volume fraction of chain α at \mathbf{r} . The subscript i refers to the different chemical groups composing the surfactant which depends on the details of the chain model being used. The averages in Equation 2 can be calculated from

$$\begin{aligned} \langle \phi_i(\mathbf{r}) \rangle &= \int \mathcal{D}\alpha P[\alpha] \phi_i(\alpha, \mathbf{r}), \\ \langle c_i(\mathbf{r}) \rangle &= \int \mathcal{D}\alpha P[\alpha] c_i(\alpha, \mathbf{r}), \end{aligned} \quad (3)$$

where $\sum_i \phi_i(\alpha, \mathbf{r})$ is the volume fraction of conformation α at \mathbf{r} . Note that the previous expression is also used to calculate the average concentration fields $\langle c_i(\mathbf{r}) \rangle$ based on the individual chain contributions $c_i(\alpha, \mathbf{r})$. The chain probabilities in Equation 3 are found to follow a Boltzmann distribution

$$P[\alpha] = \frac{e^{-H[\alpha]/kT}}{Q}, \quad (4)$$

where Q is a constant that ensures the correct normalisation of the set of probabilities and $H[\alpha]$ is the equivalent SCMF Hamiltonian for conformation α obtained from the minimisation procedure. This Hamiltonian is found to contain three main terms, namely, (i) an intramolecular term which can be calculated in an exact manner, (ii) an intermolecular energy representing the interaction of chain α with the surrounding surfactant and solvent molecules through mean molecular fields, and, (iii) a repulsive term containing the intermolecular steric repulsions. The explicit analytic form of this Hamiltonian depends on the approximations taken into account during the minimisation of F , for instance, see reference 20 for more details. Solutions of the nonlinear set of Equations 2-4 and $H[\alpha]$ provide all the required quantities for a surfactant system in an equilibrium regime, including the concentration and volume fraction fields of solvent and surfactant chains, the size distribution and the exchange chemical potential of surfactants. Moreover, the whole system of equations is affected by the chain model taken into consideration given that the number of different moieties directly affects the number of concentration and volume fraction fields as well as the number of interaction parameters. This can be observed, as will be shown later in Section 2.4, in the incompressibility condition given in Equation 2 and the SCMF Hamiltonian.

2.2. Connection with Macroscopic Quantities

We consider a system to be in equilibrium when the chemical potentials of free, μ_1 , and aggregated, (μ_2, \dots, μ_N) , surfactants are found to have the same value. Let us assume that the surfactant system behaves ideally, that is, we consider that there are no interactions between aggregates and free chains. This is a good approximation as long as the concentrations of free surfactants and aggregates are sufficiently small. The concentration of aggregated, X_N , and free, X_1 , surfactants can then be related by their corresponding standard chemical potentials μ_N^0 and μ_1^0 , respectively,

by

$$X_N = N \left[X_1 \exp \left(-\frac{\mu_N^0 - \mu_1^0}{kT} \right) \right]^N. \quad (5)$$

The above equation is derived from the mass action model and can be related to the SCMF equations. For a finite and non-Markovian set of sampling chains the following relation can be used [24],

$$\frac{\mu_N^0 - \mu_1^0}{kT} = -\log \left(\frac{V \sum_{\alpha} \exp \left(\frac{-H_N[\alpha]}{kT} \right) / W[\alpha]}{N \sum_{\alpha} \exp \left(\frac{-H_1[\alpha]}{kT} \right) / W[\alpha]} \right), \quad (6)$$

where V is the volume of the simulation box, $H_1[\alpha]$ and $H_N[\alpha]$ are the SCMF Hamiltonians for free and aggregated surfactants, respectively, and $W[\alpha]$ is the Rosenbluth and Rosenbluth weight which takes into account the bias introduced by the chain generation algorithm of self-avoiding configurations [25].

2.3. Micellization Kinetics

According to Nyrkova and Semenov [26], the micellization mechanism can be assumed to be an activation process involving collective energy barriers that may suppress or reduce certain relaxation paths depending on their values. Under this assumption, the equilibrium distribution of surfactants in aggregates in a dilute solution of surfactants and aggregates is,

$$X_N = N X_1 e^{-\mathcal{F}(N, X_1)}, \quad (7)$$

where $\mathcal{F}(N, X_1)$ is the dimensionless thermodynamic potential that contains the difference between the free energy of micellar aggregates and free chains. By relating the standard chemical potentials and the thermodynamic potential, a connection with the SCMF formalism can be obtained through the use of Equation 6 [19],

$$\mathcal{F}(N, X_1) = N \left(\frac{\mu_N^0 - \mu_1^0}{kT} \right) - (N - 1) \log X_1. \quad (8)$$

Given that the potential only depends on the size of the aggregates N and the concentration of free monomers X_1 , it can be inferred that for surfactants to associate into micellar aggregates a minimal energy regime must occur. This means that this potential ensures the existence of collective energetic barriers that when overcome allow for the formation of micelles from the free chains in solution.

2.4. Surfactant Model and Simulation Protocols

In this work we have chosen to model a block copolymer known by its trade name ED900Myr ($C_{13}H_{27}CONH-PO_3-EO_{12.5}-PO_3-NHCOC_{13}H_{27}$) where hydrophobic PO and hydrophilic EO units represent the propylene oxide ($CH(CH_3)CH_2O$) and ethylene oxide (CH_2CH_2O) groups, respectively. This system was synthesised from a polyoxyalkyleneamine by May and co-workers [8]. In this work we have modelled both hydrophobic and hydrophilic groups by beads of size σ , which is also the distance between the centres of two consecutive beads. **For simplicity, the NHCO groups are not considered in this work since the free energy of the system is not expected**

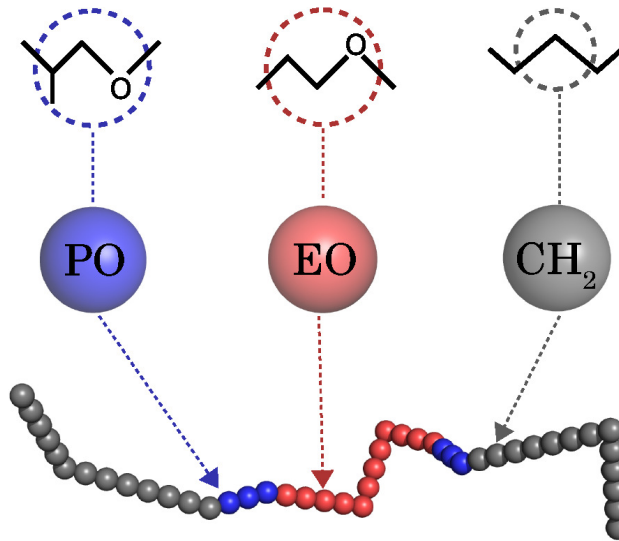


Figure 1. Schematic diagram of the coarse-grained model used in this work to model the ED900Myr surfactant where blue, red and gray beads represent PO, EO and methylene groups respectively. Top: the different chemical groups composing ED900Myr. Middle: the coarse grained beads of the different monomers. Bottom: A typical chain conformation used in the simulations.

to be significantly affected by their presence or absence compared to the 32 CH_2 and PO units. The schematic representation of the coarse-grained model used in this work can be observed in Figure 1. We take into account the chain rigidity by including Kuhn segments of length eight [18], four [20] and five [18, 20] consecutive beads for the CH_2 , PO and EO blocks, respectively. If the block length is not exactly divisible by the Kuhn segment length, we assign a block of the remaining beads as a rigid segment of shorter length. The interaction volumes are defined around every bead by a spherical shell of volume $4/3\pi(r_{int}^3 - \sigma^3)$ where the value of the interaction radius $r_{int} = 1.62\sigma$ has been adjusted to maintain a coordination number of $z = 26$. In the interior of these interactions volumes, the beads interact with the surrounding mean fields through the corresponding square-well potential whose depth ϵ depends on the cross interactions. In addition to the solvent field, we include the presence of the different chain moieties representing the hydrophobic and hydrophilic units in the concentration, volume fraction and volume interaction fields by the indexes $\{i, j\} = \{\text{CH}_2, \text{PO}, \text{EO}\}$. This, together with the volume-filling constraint, explicitly introduces the configurational details of the chain model as can be observed on expanding Equations 2 and 3.

Taking into account the relationship between the Flory-Huggins and the energetic parameters, $\epsilon_{i,j} = kT\chi_{i,j}/z$, and that the interactions are symmetric, $\chi_{i,j} = \chi_{j,i}$, the SCMF Hamiltonian is found to be of the form

$$H[\alpha] \approx u_{\text{intra}}(\alpha) + (N - 1) \frac{kT}{z} \int d\mathbf{r} \sum_{i \neq j} \chi_{i,j} \Phi_i(\alpha, \mathbf{r}) \langle c_j(\mathbf{r}) \rangle + \frac{kT}{z} \int d\mathbf{r} \sum_i \chi_{i,S} \Phi_i(\alpha, \mathbf{r}) c_S(\mathbf{r}) \quad (9)$$

$$- kT \int d\mathbf{r} \frac{\log \phi_S(\mathbf{r})}{v_S} \sum_i \phi_i(\alpha, \mathbf{r}).$$

The first term on the right hand side is the intramolecular energy of configuration α and can be calculated in an exact way. In this work this value is calculated as the product between the number of non-consecutive EO-PO, CH_2 -EO and CH_2 -PO contacts and the Flory-Huggins $\chi_{\text{EO,PO}}$, $\chi_{\text{CH}_2,\text{EO}}$ and $\chi_{\text{CH}_2,\text{PO}}$. The second and third terms represent the intermolecular interactions of α ,

Table 1. Energetic and structural parameters in the coarse-grained model for ED900Myr at 25 °C.

Diameter (σ)	1.0
Bond length (σ)	1.0
Interaction radius (σ)	1.62
EO-S interaction parameter ($\chi_{EO,S}$)	0.5
PO-S interaction parameter ($\chi_{PO,S}$)	1.77
CH ₂ -S interaction parameter ($\chi_{CH_2,S}$)	3.984
CH ₂ -PO interaction parameter ($\chi_{CH_2,PO}$)	0
CH ₂ -EO interaction parameter ($\chi_{CH_2,EO}$)	0.34
PO-EO interaction parameter ($\chi_{EO,PO}$)	0.08

through its interaction volumes $\Phi_i(\alpha, \mathbf{r})$ with the mean concentration fields of the chains $\langle c_j(\mathbf{r}) \rangle$ and solvent $c_S(\mathbf{r})$ molecules together with their energetic parameters $\chi_{i,j}$ and $\chi_{i,S}$. In Table 1 the structural and energetic coarse-grained parameters adopted to model the surfactant ED900Myr are shown. In this case we have a total of four different chemical species which gives rise to 6 independent interactions [27]. This is a good approximation for incompressible systems such as the one studied in this work where the total number of contacts is approximately constant. The interaction parameters between CH₂, EO and the solvent species were given by Gezae and co-workers for a set of nonionic polyethylene oxide alkyl ether diblock surfactants at a temperature of 25 °C [18]. In a similar way, the energetic parameters between EO, PO and solvent units were fitted in a previous work for poly(ethylene oxide)-poly(propylene oxide)-poly(ethylene oxide) triblock copolymers at a temperature of 37 °C [20]. To obtain the Flory-Huggins energetic values to model ED900Myr at our target temperature of 25 °C, we performed an optimisation procedure based on the minimisation of an objective function which takes into account the difference between the experimental and calculated CMCs [20]. In this case, it was only necessary to fit the energetic parameters for PO-EO and PO-S interactions for this new temperature. We used as target values the experimental CMC values of 1×10^{-3} mol/L and 8.8×10^{-3} mol/L for Pluronics P94 (EO₂₁PO₄₉EO₂₁) and L64 (EO₁₃PO₃₀EO₁₃), respectively, reported by Lopes and Loh [28] for a temperature of 25 °C. These surfactants were selected given the considerable difference in the number of their hydrophobic units which allows for the impact of the PO-S interaction to be more accurately estimated. The initial estimates for the parameters were taken from our previous work at 37 °C [20] to finally obtain the fitted values shown in Table 1. In addition, and due to the lack of available experimental data, we assume a value of $\chi_{CH_2,PO} = 0$ as a reasonable estimate given that $\chi_{CH_2,EO}$ is already relatively small and the PO group is expected to be more hydrophobic than the EO group.

The SCMF simulations are separated into two stages. First, a set of non-overlapping sampling chains $\{\alpha\}$ is generated inside a simulation box using the Rosenbluth & Rosenbluth algorithm [25]. From these configurations the volume fractions $\phi_i(\alpha, \mathbf{r})$ and interaction volumes $\Phi_i(\alpha, \mathbf{r})$ can be estimated for every conformation, α , via a Monte Carlo integration method. Furthermore, the intramolecular energy $u_{\text{intra}}(\alpha)$ and the concentrations $c_i(\alpha, \mathbf{r})$ can be calculated. Second, by the solution of the SCMF equations, the mean molecular fields $\langle c_i(\mathbf{r}) \rangle$ and $\langle \phi_i(\mathbf{r}) \rangle$ are found by solving Equations 3 which in turn requires the knowledge of $\phi_S(\mathbf{r})$, $P[\alpha]$ and the SCMF Hamiltonian $H[\alpha]$ that are calculated from Equations 2, 4 and 9. As can be observed, the whole process is self-consistent and is solved in an iterative manner.

In this work we assume that the aggregates have a one-dimensional spherical symmetry by dividing the simulation box into concentric spherical shells with a width in the range of $1.0\sigma - 1.2\sigma$. Different simulation boxes of sizes $(50\sigma)^3$, $(60\sigma)^3$ and $(70\sigma)^3$ were used to help check for the presence of finite size effects. Sampling sets $\{\alpha\}$ of 1×10^7 conformations were generated to run the simulations in 24-core AMD workstations with RAM memories of 32 GB.

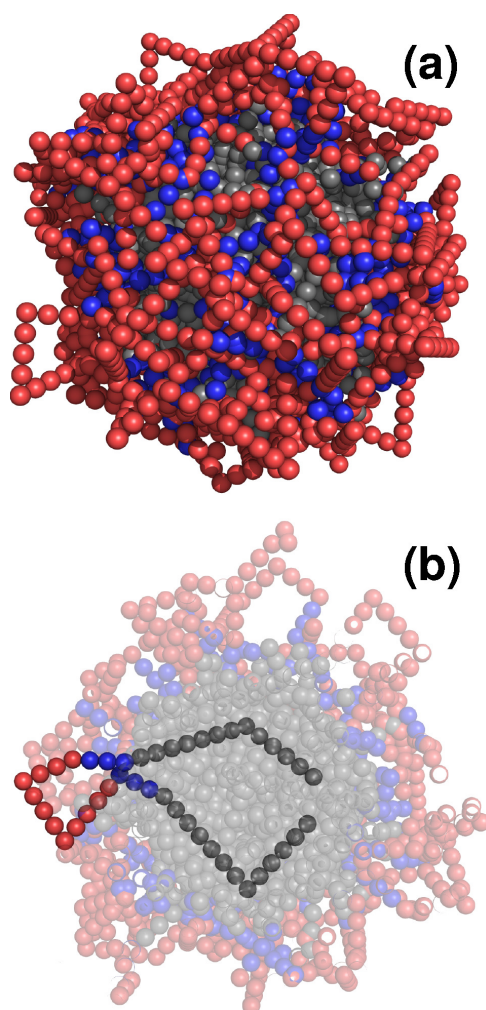


Figure 2. Schematic diagram of the surfactant micelles obtained from the set of most probable conformations of the chains. (a) Spherical micelle with $N = 100$ for ED900Myr. (b) Cross-section view of the micellar aggregate where the chain with the highest probability conformation is highlighted. Red beads represent the hydrophilic EO groups and the hydrophobic PO and CH_2 units are represented by blue and gray beads, respectively.

3. Results and Discussion

Our simulations reveal the presence of spherical micellar aggregates whose hydrophobic units are placed in the interior of the micelle to minimise contact with the water solvent molecules. A snapshot of the most probable configurations comprising a spherical micelle of aggregation number $N = 100$, can be observed in Figure 2(a). A cross-section of the same micelle with the highest probability conformation highlighted is given in Figure 2(b). These snapshots are merely schematic and do not correspond to a real micelle given the mean-field nature of the SCMF theory. The ED900Myr surfactant has a central hydrophilic block surrounded by exterior hydrophobic blocks which force the surfactant to make a loop to place both these hydrophobic blocks in the micellar core. The PO groups, which are positioned between the central hydrophilic and exterior CH_2 block and have a weaker interaction with the solvent in comparison with the CH_2 groups, are found in a shell around the hydrophobic core. In contrast, the more favourable interactions of water solvent molecules with the EO hydrophilic groups promotes the formation of the EO units in a final exterior shell around the more hydrophobic groups to prevent their contact with the water medium. In Figure 3 the volume fraction profile as a function of the radius of the different

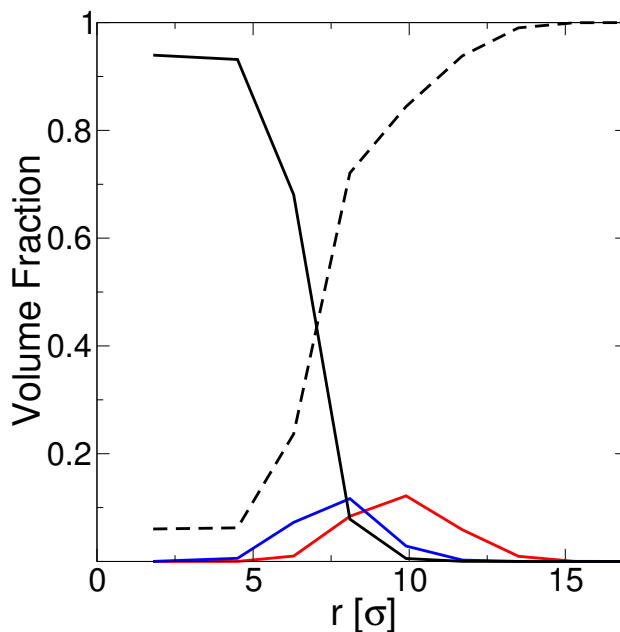


Figure 3. Average volume fraction profile as a function of radius, r , for a ED900Myr micelle with an aggregation number $N = 100$. The black line represents the volume fraction of methylene groups, blue and red lines correspond to the presence of PO and EO units, respectively, while the dashed line represents the solvent profile.

surfactant groups, $\{\langle\phi_{\text{CH}_2}(\mathbf{r})\rangle, \langle\phi_{\text{PO}}(\mathbf{r})\rangle, \langle\phi_{\text{EO}}(\mathbf{r})\rangle\}$, and solvent, $\langle\phi_{\text{S}}(\mathbf{r})\rangle$, is given for a micelle of aggregation number $N = 100$. As can be seen, the CH_2 groups occupy a maximum of about 94% of the available volume in the centre of the micelle to then decrease to eventually reach its bulk value of 0.02% after 11σ . In contrast, the solvent has the opposite trend and in the bulk occupies close to 100% of the solution and reaches a minimum and almost constant value of 6% in the micelle core. The cores of the micelles found in our simulations are therefore not dry as we find a significant fraction of solvent to be present. The volume fraction of hydrophobic PO units increases smoothly away from the micelle centre to reach a maximum value close to 12% at 8σ of the available volume to later decrease. This behaviour is similar to the one corresponding to the more hydrophilic EO corona which exhibits a much larger contact with the solvent molecules as it forms the most external shell of the micelle with a maximum at 10σ .

However, as can be observed in Figure 4, when the aggregation number of the micelle is increased to $N = 245$ the hydrophobic methylene units are no longer able to occupy the centre of the micellar core. As expected, as the micelle becomes larger, at some point the length of the methylene blocks is not sufficient to reach the entire inner region. In consequence, the volume fraction of water increases in the centre in order to occupy the available space in the hydrophobic core. The surfactant chains are composed of five blocks with two hydrophobic ends. This means that there is a high entropic cost needed to accommodate the hydrophobic blocks in the centre of the micelle because of the looping of the surfactant. In addition, the chains have a certain rigidity according to the already quoted Kuhn segments which make it even more difficult to form a loop. The thicknesses of the PO and EO shells remain relatively constant for the two micelles at $\sim 5\sigma$ and $\sim 6\sigma$, respectively, as can be observed in Figures 3 and 4. This is because the imposed rigidity and number of segments representing these blocks lead them to be relatively stretched. In contrast, the fraction of occupied volume by these blocks in the larger micelle is almost double, reaching approximately 20% of the available space.

Experimental data for ED900Myr [8] reveal the existence of spherical micelles with a diameter of 7 nm. However, no information on the aggregation number of the micelles could be found so it is

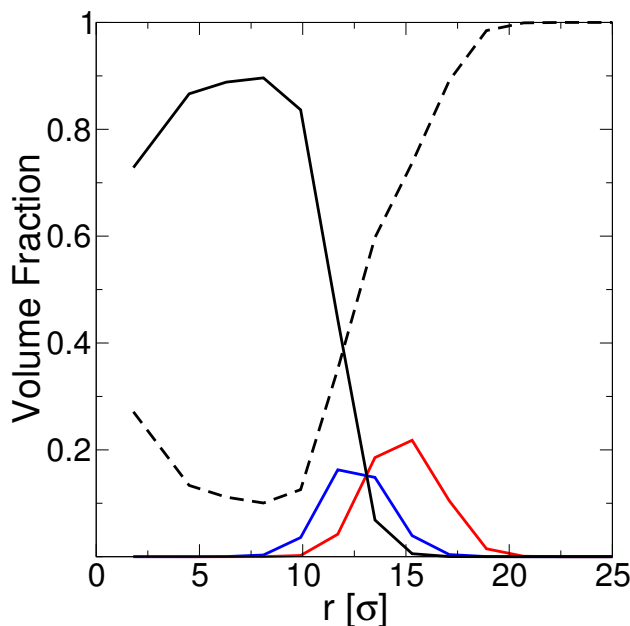


Figure 4. Average volume fraction profile as a function of radius, r , for a ED900Myr micelle with an aggregation number $N = 458$. The black line represents the volume fraction of methylene groups, blue and red lines correspond to the presence of PO and EO units, respectively, while the dashed line represents the solvent profile.

difficult to compare directly with the experimental data. The aggregation numbers of $N = 100$ and $N = 458$ shown in Figures 3 and 4 were chosen as they correspond to two local minima in the equilibrium state. From Figures 3 and 4 we obtain from our SCMF calculations radii of 12.5σ and 17.5σ , respectively. If we assume that $\sigma = 0.5$ nm as suggested in the literature [29] we obtain diameters in the range 12.5-17.5 nm which is clearly far from the value reported by experiments. It should be noted that each CH_2 unit in our simple coarse-grained model was taken to have the same size as the EO or PO groups. The use of $\sigma = 0.5$ nm is without a doubt too large and a much smaller value of half this amount would fit in better with the experimental observation, particularly for the smaller aggregate. This is a rough approximation particularly when analysing the structural properties of the micelles however the micellar free energy is expected to be less affected by this assumption as the energetic and entropic contributions should be reasonably well modelled. In any case, the value of $\sigma = 0.5$ nm should be valid for both PO and EO units. As mentioned above, the thickness of the PO shell appears to be almost independent of the size of the micelle and is found to be roughly $5\sigma \approx 2.5$ nm. Again, this value is much larger than the reported experimental value of 1 nm. Another property that is useful to compare in micellar systems is the aggregate size distribution. Unfortunately, this value was not reported.

To calculate the CMC, we start from the evaluation of the thermodynamic potential in Equation 8 from the SCMF simulations and Equation 6. In particular, we compute $\mathcal{F}(N_{agg}, CMC) = 0$, and, $\partial\mathcal{F}(N, CMC)|_{N=N_{agg}} = 0$ giving rise to association, F_a , and dissociation, F_d potentials. These two potentials are responsible for the formation and dissociation of micelles by overcoming the associated energetic barriers, as shown in Figure 5. As can be observed, F_a is defined as the maximum of the thermodynamic function $\mathcal{F}(N, X_1)$ for $X_1 = CMC$, and corresponds to the energetic barrier to be overcome by the surfactants to associate into micelles. On the contrary, F_d is defined as the barrier to be surpassed for surfactants leaving micelles. Both are dependent on the enthalpic/entropic balance influenced by the free monomer concentration according to Equation 8. Based on this, three scenarios are possible [19, 26]. First, association of surfactants

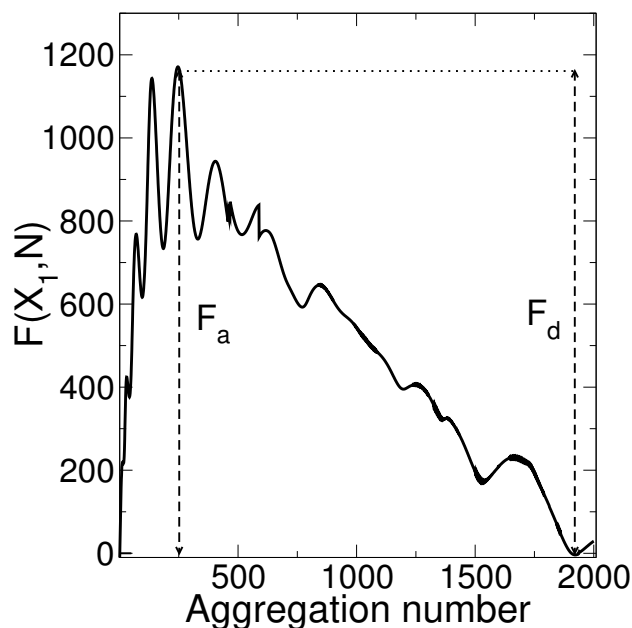


Figure 5. Thermodynamic Potential $\mathcal{F}(N, X_1)$ as a function of aggregation number in the equilibrium regime where $F_a = F_d$ and $X_1 = \text{CMC}$.

into micelles when the free monomer concentration is higher than the equilibrium CMC ($F_a < F_d$). Second, expulsion of surfactants from micellar aggregates when the free surfactant concentration is below the CMC ($F_a > F_d$). Third, an equal rate of association and dissociation of surfactants leaving or entering into micelles. In this case there is no net change and the number of micelles is kept constant when the free surfactant concentration is the same as the CMC, ($F_a = F_d$).

In addition to the global maximum energy barrier commented on in the previous paragraph, an interesting series of local minima and maxima for the thermodynamic potential can be observed. The presence of these minima can be expected to give rise to metastable micelles, subject to the time scale applied in order for the system to stay within a given local minima. These non-equilibrium structures can doubtlessly be related to the formation of *premicelles* which have been reported by other authors in the literature. Only a few simulation studies have been devoted to study the presence of premicelles and these studies have been restricted to relatively short surfactants because of the spatial and temporal limitations found when equilibrating the systems [30]. As a consequence, the nature of the physical mechanisms responsible for the presence of these structures is still unclear from a microscopic point of view however our work shows that these are likely to be metastable aggregates whose stability depends on the time scale used in the simulations or experiment.

In general, the characteristic time for micellization to occur is defined by $T_a = T_0 e^{F_a}$, where $T_0 = 6\pi\eta R^3/(N_{agg}kT)$ is the elementary association time [26], $\eta = 8.91 \times 10^{-4} \text{kg/m.s}$ is the viscosity of water at 298.15K, $R = 6.15 \text{nm}$ is the hydrodynamic radius obtained from SCMF simulations for free chains, $kT = 4.11 \times 10^{-3} \text{kg.nm}^2/\text{s}^2$ and N_{agg} the aggregation number in the equilibrium regime. According to Figure 5, $N_{agg} = 1922$, in consequence $T_0 = 4.9 \times 10^{-10} \text{s}$. In addition, $F_a \approx 1171$ which corresponds to an association time $T_a \sim e^{1171}$ being an astronomically large time scale for the equilibrium micellization process to occur with the CMC of $\sim 10^{-17} \text{mol/L}$. As already mentioned, the equilibrium CMC was calculated as the free monomer concentration X_1 that ensures that the association and dissociation potentials have the same value based on Equation 8 and the standard chemical potential difference obtained from the SCMF simulations. This CMC value that we find from our SCMF calculations is many orders of magnitude lower

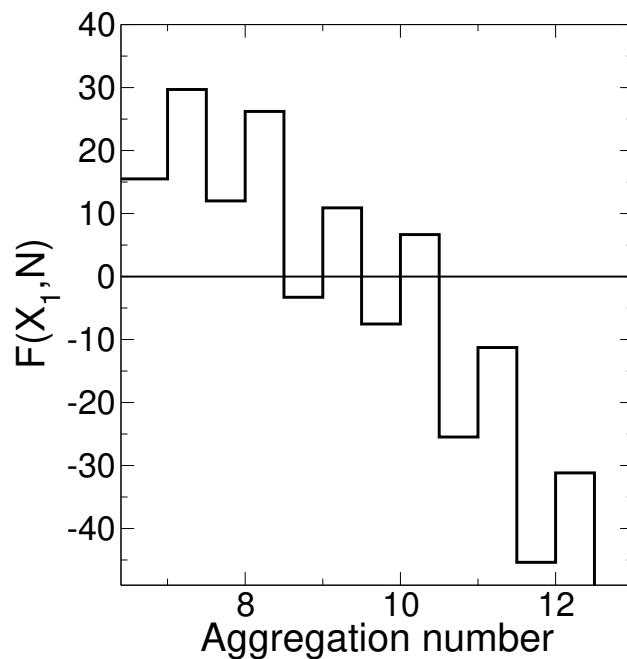


Figure 6. Thermodynamic potential $\mathcal{F}(N, X_1)$ for $X_1 = 1.1 \times 10^{-6}$ mol/L.

than the experimental values reported for similar nonionic gemini surfactant [21] systems with a comparable number of hydrophobic methylene units. It is also orders of magnitude lower than other diblock and triblock block copolymer surfactants [31]. In general, reported experimental CMCs for the most hydrophobic surfactants lie in the range $10^{-8} - 10^{-6}$ mol/L [22].

In order to understand this substantial difference between our calculated CMCs compared to the reported experimental ones, it is useful to consider the definition of apparent CMCs made by Nyrkova and Semenov [26], CMC^{app} , which take into consideration the laboratory time scales used in measuring experimental CMCs. In the CMC^{app} the number of free surfactants X_1 is increased arbitrarily in the thermodynamic potential in Equation 8 which forces the aggregation to occur at much smaller time scales. As a result, F_a decreases to an apparent value, F_a^{app} , that causes micellization to occur in the available experimental time $T_a^{app} = T_0 e^{F_a^{app}}$. In essence, by taking an initial estimate of T_a^{app} , it is possible to calculate the corresponding value of F_a^{app} and hence the apparent free monomer concentration CMC^{app} .

An entropic contribution can be included in the association energy barrier to take into account the non-continuous nature of the aggregation mechanism, namely that a whole surfactant has to be added at one time to a micelle. Two processes are proposed in the elementary entrance of a surfactant into an aggregate. In the first place, there is a slow approach of the surfactant to the inner core, and second, a diffusion of the hydrophobic blocks of the surfactant into the aggregate core. If the first scenario is taken as the dominant one [26], then the thermodynamic potential also includes the term $\mathcal{F}(N + 1/2, X_1) = \mathcal{F}(N, X_1) - \log \Phi_1$, where $\Phi_1 = X_1 v_p$ and v_p is the surfactant molecular volume. This term affects the calculation of the time necessary to form micelles for this regime given that the association barrier is taken from $F_a^{app} = \max\{\mathcal{F}(N + 1/2, X_1)\}$. In Figure 6 the behaviour of the association barrier is given with an association time $T_a^{app} = 1$ h. From our calculations $F_a^{app} \approx 30$ for a free surfactant concentration X_1 which corresponds to $\text{CMC}^{app} = 1.1 \times 10^{-6}$ mol/L.

As can be observed, there is a difference of 11 orders of magnitude between the equilibrium CMC and CMC^{app} . This huge difference shows the importance of the kinetic effects in the micellization process for the ED900Myr surfactant. [It should be possible to observe these kinetic effects](#)

experimentally, at least indirectly, for surfactant systems which are controlled by these processes. For example, experimental observations of the CMC should show an unexpected behaviour when either the experimental timescale is raised or the surfactant solvophobic length is sufficiently increased. In the first case, the CMC is expected to decrease when the experimental timescale is increased [19, 22, 26]. Although few experimental articles comment specifically on these effects, surface tension measurements have been reported for stilbene-based geminis [32] where a decrease of 2-fold of the CMC was found for samples aged over 24 hours at different temperatures. Similarly, samples of Pluronic P85 aged over 1 or 16 hours are found to exhibit a decrease of one order of magnitude [33]. It should be noted, however, that the authors suggest that this difference was caused by experimental effects of the fluorescence measurements due to the presence of supramolecular complexes of the DPH probe.

In the second case, the CMC is expected to decrease exponentially with respect to the length of the hydrophobic block of the surfactant. If kinetic effects appear then the CMC is expected to deviate from this exponential decay and saturate at a constant value. This statement is supported by the fact that no CMCs have been reported below approximately 10^{-8} mol/L [22]. In addition, in the case of bis quaternary ammonium surfactants, a saturation of the CMC was found at 10^{-5} - 10^{-6} mol/L [34, 35]. Furthermore, for dimeric poly(ethylene oxide) surfactants the CMCs were found to saturate at $10^{-6} - 10^{-7}$ mol/L [21]. In contrast, shorter surfactants with higher CMC values above 10^{-5} mol/L are not expected to exhibit non-equilibrium effects on typical experimental timescales of an hour as has been corroborated from theoretical [12] and simulation studies [19, 20]

It is also interesting to note that our predicted value CMC^{app} when a time scale of one hour is used is surprisingly close to the experimental one reported by surface tension measurements [8] of 1×10^{-6} mol/L, although at a temperature of 20 °C. This temperature differs from the 25 °C used in this work to optimise the energetic parameters, however, we do not expect a difference of 5 °C to significantly affect our CMC value. Previous experimental data used to compare with SCMF simulations for analogous diblock surfactants reveal only slight changes over a wide range of temperature [31]. Furthermore, the PO units give a relatively small free energy contribution in comparison with the methylene blocks given their larger number of units and the higher value of the repulsive interaction. As a result, a difference of 5 °C is not expected to significantly change the calculated CMC value and the good agreement between our simulated CMC to the experimental value is expected to be conserved.

4. Conclusions

In this work we have presented a coarse-grained model for a polyoxyalkyleneamine based surfactant ED900. The energetic parameters for interactions between methylene, ethylene oxide and water units were taken from our published previous models, whilst the cross terms with propylene oxide species were optimised using a previously developed fitting procedure. Our calculations reveal the presence of spherical micelles whose structure agrees qualitatively with available experimental data where the surfactants adopt loop configurations to form a hydrophobic methylene core surrounded by less hydrophobic PO units and finally a corona composed of hydrophilic EO blocks. The coarse-grained model could be further improved particularly in the treatment of the methylene groups since their relatively much smaller size is not taken into account, [or in the addition of the NHCO groups which were not included in the present model](#). Although such improvements would be expected to enhance the structural properties of the micelle such as the physical size of the core or the aggregation number, the free energy estimates and hence the CMC should not be significantly affected.

The calculated CMC value was found to deviate from the experimental one by several orders of magnitude. In addition, the very low numerical value of the CMC indicates, according to the kinetic

theory of micellization, that astronomical times must be needed to observe the equilibrium CMCs. The formation of aggregates on a shorter time scale, typical of the ones available in a laboratory, requires the use of surfactant concentrations well above the equilibrium ones. In other words, non-equilibrium aggregates can be forced to form at a chosen time scale by arbitrarily increasing the free surfactant concentration giving rise to an apparent CMC for ED900Myr close to 10^{-6} mol/L on a time scale of one hour. Strikingly, this apparent CMC is very close to the reported experimental value.

5. Acknowledgements

F.A.G.D. acknowledges financial support from the URV through his Ph.D. scholarship. The authors acknowledge financial assistance from the Ministerio de Economía y Competitividad of the Spanish Government (Grant CTQ2014-52687-C3-1-P).

References

- [1] Bombelli C, Giansanti L, Luciani P, et al. Gemini surfactant based carriers in gene and drug delivery. *Curr Med Chem*. 2009;16:171–183.
- [2] Sineva A, Parfenova A, Fedorova A. Adsorption of micelle forming and non-micelle forming surfactants on the adsorbents of different nature. *Colloids Surf, A*. 2007;306:68–74.
- [3] Erdem A, Ngwabebhoh F, Yildiz U. Synthesis, characterization and swelling investigations of novel polyetheramine-based hydrogels. *Polym Bull*. 2017;74:873–893.
- [4] Lu B, Vayssade M, Miao Y, et al. Physico-chemical properties and cytotoxic effects of sugar-based surfactants: Impact of structural variations. *Colloids Surf, B*. 2016;145:79–86.
- [5] Vemula P, John G. Crops: A green approach toward self-assembled soft materials. *Acc Chem Res*. 2008;41:769–782.
- [6] Wan Y, Zhao D. On the controllable soft-templating approach to mesoporous silicates. *Chem Rev (Washington, DC, U S)*. 2007;107:2821–2860.
- [7] Wan Y, Shi Y, Zhao D. Designed synthesis of mesoporous solids via nonionic-surfactant-templating approach. *Chem Commun (Cambridge, U K)*. 2007;:897–926.
- [8] May A, Pasc A, Stébé MJ, et al. Tailored jeffamine molecular tools for ordering mesoporous silica. *Langmuir*. 2012;28:9816–9824.
- [9] Stébé M, Emo M, Forny-Le Follotec A, et al. Triblock siloxane copolymer surfactant: Template for spherical mesoporous silica with a hexagonal pore ordering. *Langmuir*. 2013;29:1618–1626.
- [10] Riachy P, Lopez G, Emo M, et al. Investigation of a novel fluorinated surfactant-based system for the design of spherical wormhole-like mesoporous silica. *J Colloid Interface Sci*. 2017;487:310–319.
- [11] Nagarajan R, Ruckenstein E. Theory of surfactant self-assembly. a predictive molecular thermodynamic approach. *Langmuir*. 1991;7:2934–2969.
- [12] Camesano T, Nagarajan R. Micelle formation and cmc of gemini surfactants: A thermodynamic model. *Colloids Surf, A*. 2000;167:165–177.
- [13] Jusufi A, Hynninen AP, Panagiotopoulos A. Implicit solvent models for micellization of ionic surfactants. *J Phys Chem B*. 2008;112:13783–13792.
- [14] Sanders S, Panagiotopoulos A. Micellization behavior of coarse grained surfactant models. *J Chem Phys*. 2010;132.
- [15] Levine B, Lebard D, Devane R, et al. Micellization studied by gpu-accelerated coarse-grained molecular dynamics. *J Chem Theory Comput*. 2011;7:4135–4145.
- [16] De Bruijn V, Van den Broeke L, Leermakers F, et al. Self-consistent-field analysis of poly(ethylene oxide)-poly(propylene oxide)-poly(ethylene oxide) surfactants: Micellar structure, critical micellization concentration, critical micellization temperature, and cloud point. *Langmuir*. 2002;18:10467–10474.
- [17] Mackie A, Panagiotopoulos A, Szleifer I. Aggregation behavior of a lattice model for amphiphiles. *Langmuir*. 1997;13:5022–5028.

- [18] Gezae Daful A, Baulin VA, Bonet Avalos J, et al. Accurate critical micelle concentrations from a microscopic surfactant model. *J Phys Chem B*. 2011;115:3434–3443.
- [19] García Daza FA, Mackie AD. Low critical micelle concentration discrepancy between theory and experiment. *J Phys Chem Lett*. 2014;5:2027–2032.
- [20] García Daza FA, Colville AJ, Mackie AD. Mean-field coarse-grained model for poly(ethylene oxide)-poly(propylene oxide)-poly(ethylene oxide) triblock copolymer systems. *Langmuir*. 2015;31:3596–3604.
- [21] FitzGerald PA, Carr MW, Davey TW, et al. Preparation and dilute solution properties of model gemini nonionic surfactants. *J Colloid Interface Sci*. 2004;275:649–658.
- [22] Mok M, Thiagarajan R, Flores M, et al. Apparent critical micelle concentrations in block copolymer/ionic liquid solutions: Remarkably weak dependence on solvophobic block molecular weight. *Macromolecules*. 2012;45:4818–4829.
- [23] Ben-Shaul A, Szeleifer I, Gelbart W. Chain organization and thermodynamics in micelles and bilayers. i. theory. *J Chem Phys*. 1985;83:3597–3611.
- [24] Al-Anber ZA, Avalos JB, Mackie AD. Prediction of the critical micelle concentration in a lattice model for amphiphiles using a single-chain mean-field theory. *J Chem Phys*. 2005;122:104910.
- [25] Rosenbluth MN, Rosenbluth AW. Monte carlo calculation of the average extension of molecular chains. *J Chem Phys*. 1955;23:356–359.
- [26] Nyrkova IA, Semenov AN. On the theory of micellization kinetics. *Macromol Theory Simul*. 2005;14:569–585.
- [27] Patti A, Mackie A, Siperstein F. Monte carlo simulation of self-assembled ordered hybrid materials. *Langmuir*. 2007;23:6771–6780.
- [28] Lopes J, Loh W. Investigation of self-assembly and micelle polarity for a wide range of ethylene oxide-propylene oxide-ethylene oxide block copolymers in water. *Langmuir*. 1998;14:750–756.
- [29] Rubinstein M, Colby RH. *Polymer Physics*. 1st ed. Oxford: Oxford University Press; 2003.
- [30] LeBard DN, Levine BG, DeVane R, et al. Premicelles and monomer exchange in aqueous surfactant solutions above and below the critical micelle concentration. *Chem Phys Lett*. 2012;522:38–42.
- [31] Rosen MJ, Kunjappu JT. *Micelle formation by surfactants*. John Wiley & Sons, Inc.; 2012. Chapter 3; p. 123–201.
- [32] Menger FM, Littau CA. Gemini surfactants: a new class of self-assembling molecules. *J Am Chem Soc*. 1993;115:10083–10090.
- [33] Kabanov AV, Nazarova IR, Astafieva IV, et al. Micelle formation and solubilization of fluorescent probes in poly(oxyethylene-b-oxypropylene-b-oxyethylene) solutions. *Macromolecules*. 1995;28:2303–2314.
- [34] Song LD, Rosen MJ. Surface properties, micellization, and premicellar aggregation of gemini surfactants with rigid and flexible spacers. *Langmuir*. 1996;12:1149–1153.
- [35] Rosen MJ, Mathias JH, Davenport L. Aberrant aggregation behavior in cationic gemini surfactants investigated by surface tension, interfacial tension, and fluorescence methods. *Langmuir*. 1999;15:7340–7346.